Communications in Physics, Vol. 35, No. 3 (2025), pp. 245-256
DOI: https://doi.org/10.15625/0868-3166/22700

Characterization of Au/TiO_2 nanocomposite and its application to photocatalytic degradation of methylene blue

Pham Minh Thuy[1,2,3], **Vu Duc Chinh**[1,2,†], **Chu Thi Thu Hien**[3]

[1]*Institute of Materials Science, Vietnam Academy of Science and Technology, Hanoi, Vietnam*

[2]*Graduate University of Science and Technology, Vietnam Academy of Science and Technology, Ha Noi, Viet Nam*

[3]*Department of Chemistry, Faculty of Building Materials, Hanoi University of Civil Enginerring (HUCE), Giai Phong, Bach Mai, Hanoi, Vietnam*

E-mail: [†]chinhvd@ims.vast.ac.vn

Received 14 April 2025; *Accepted for publication 20 July 2025*; *Published 29 July 2025*

Abstract. *Au nanoparticles were deposited on the surface of TiO_2 particles using a photochemical reduction method. This modification creates a surface plasmon effect that enhances the local light intensity at the interface of Au and TiO_2 nanoparticles. Au/TiO_2 nanocomposites with varying Au content (0.5%, 1%, 3%, and 5%) were synthesized, resulting in Au nanoparticles of approximately 2 nm in size uniformly distributed on the TiO_2 surface, forming composite particles of the size ranging from 100 nm to 150 nm. The prepared samples were characterized by infrared spectroscopy (FT-IR), X-ray diffraction (XRD), energy dispersive X-ray spectroscopy (EDX), UV-Vis absorption spectra, photoluminescence spectra and X-ray photoelectron spectroscopy (XPS). The photocatalytic activity of the nanocomposites was evaluated. Compared with pure TiO_2, Au/TiO_2 exhibited higher activities for methylene blue decomposition. The rate constants of pseudo-first-order kinetics for Au-modified TiO_2 with Au contents of 0.5%, 1%, 3%, and 5% were 0.0456, 0.0579, 0.0536, and 0.0484 min^{-}, respectively. These values are 1.66, 2.11, 1.95, and 1.76 times higher than that of unmodified TiO_2.*

Keywords: Au/TiO_2 nanocomposite; photocatalysis; methylene blue degradation.

Classification numbers: 12.60.Rc; 81.07.-b; 81.16.Be.

1. Introduction

Noble metal nanoparticles (NMNPs) have garnered significant attention from the scientific community in recent decades due to their unique physicochemical properties arising from their size and surface plasmon resonance (SPR) [1–6]. While advancements in synthesis techniques have

enabled the fabrication of NMNPs with tailored shapes, sizes, and compositions, a comprehensive understanding of their intricate behavior and synergistic interactions within composite materials remains an active area of research. Among the noble metals, gold (Au) nanoparticles (NPs) stand out due to their exceptional chemical stability, biocompatibility, and strong SPR absorption in the visible light region, making them promising candidates for various applications, including catalysis, sensing, and biomedicine [7–12].

In the realm of environmental remediation, photocatalysis has emerged as a sustainable and efficient technology for the degradation of organic pollutants. Titanium dioxide (TiO_2), a well-established semiconductor photocatalyst, has been extensively studied due to its low cost, chemical inertness, and high photocatalytic activity under UV irradiation. However, the practical application of pristine TiO_2 is often limited by its wide band gap, leading to UV-only activation, and the rapid recombination of photogenerated electron-hole pairs, which diminishes its quantum efficiency [13–16].

To overcome these limitations, significant research efforts have focused on surface modification of TiO_2 with NMNPs, particularly Au NPs, has proven to be an effective strategy for enhancing its photocatalytic performance. The incorporation of Au NPs can induce several beneficial effects: (i) the SPR of Au NPs can enhance visible light absorption and promote the generation of electron-hole pairs in TiO_2; (ii) Au NPs can act as electron traps, effectively reducing the recombination rate of photogenerated charge carriers; and (iii) the intimate contact between Au and TiO2 can facilitate interfacial charge transfer, further boosting the photocatalytic efficiency [17, 18].

Despite the well-documented benefits of Au/TiO_2 nanocomposites, a thorough understanding of the relationship between the synthesis method, the resulting physicochemical properties (e.g., size, dispersion, electronic state of Au NPs), and the photocatalytic activity towards specific pollutants remains crucial for optimizing their performance. Different synthesis routes, such as sputtering, chemical reduction, and laser ablation, can lead to variations in the morphology and electronic structure of the Au NPs, which in turn can significantly influence the photocatalytic degradation efficiency. Among these methods, photochemical reduction offers advantages such as simplicity, mild reaction conditions, and the potential for controlled nanoparticle growth.

This work aims to contribute to the fundamental understanding and optimization of Au/TiO_2 nanocomposites for environmental applications. By employing a facile chemical reduction method for the synthesis of Au-modified TiO_2, this study seeks to meticulously characterize the resulting material using a comprehensive suite of techniques, including field emission scanning electron microscopy with energy dispersive spectroscopy (FE-SEM with EDS) to investigate morphology and composition, Fourier transform infrared spectroscopy (FT-IR) to analyze surface functional groups, X-ray diffraction (XRD) to determine the crystalline structure, UV-Vis absorption spectroscopy to evaluate optical properties, and X-ray photoelectron spectroscopy (XPS) to elucidate the surface chemical states of the constituent elements. Furthermore, this research will directly address the practical relevance of the synthesized nanocomposite by evaluating its photocatalytic performance in the degradation of methylene blue (MB), a common and persistent organic pollutant in wastewater. By correlating the physicochemical characteristics of the Au/TiO_2 nanocomposite with its photocatalytic activity, this study intends to provide valuable insights for the rational design and development of highly efficient photocatalytic materials for environmental remediation.

2. Experiment

2.1. Synthesis of materials

TiO_2 was synthesized using the sol – gel method. The procedure began with the hydrolysis of Tetrabutyl titanate (TBOT) and absolute alcohol in distilled water. Then, the solution was continuously stirred for about 2 hours at room temperature, and it was ensured that the temperature did not change significantly during the hydrolysis process (Fig. 1).

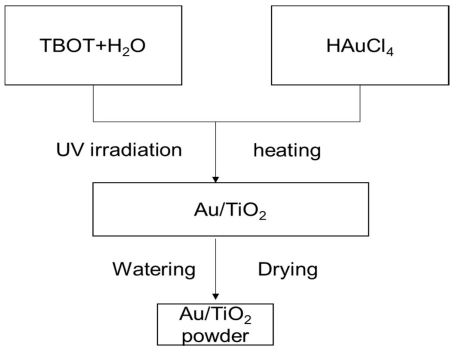

Fig. 1. Fabrication diagram of Au/TiO_2 nanocomposite material.

In the next process, an amount of $HAuCl_4$ solution corresponding to Au mass % is 0.5%; 1%; 3% and 5% were added to the prepared mixture containing TiO_2 and water. After that, the entire solution will be exposed to UV light for 3 hours to conduct a reaction to reduce Au^{3+} ions into Au nanoparticles on the surface of TiO_2. The resulting powder is Au/TiO_2 material that will be separated by centrifugation at a speed of 4000 rpm and dried at a temperature of 60^{o}C until the mass remains constant. After the drying process ended, the sample would be finely ground using a ceramic mortar to separate the particles from each other. Finally, the material was stored in an esiccator and used for the next steps in the research process.

Images of TiO_2 nanomaterial and Au/TiO_2 nanocomposites are shown in Fig. 2. TiO_2 nanomaterial is white, after adding $HAuCl_4$ precursor, the solution has a light yellow color. After the mixture was exposed to UV light, the color of the TiO_2 material began to change, showing that the reduction of Au^{3+} ions into Au^0 began to form. Depending on the content of Au^{3+}, the color of the resulting composite material will be different. The $Au0.5\%/TiO_2$ sample with the smallest Au content has pinkish color, the $Au1\%/TiO_2$ sample has purple-pink color, the $Au3\%/TiO_2$ sample has dark purple color, and the $Au5\%/TiO_2$ sample has blue gray color. This change in color shows that the content of the Au coating on the TiO_2 surface increases in the order of $Au0.5\%/TiO_2$ to $Au5\%/TiO_2$ samples.

2.2. Physical methods to study material characteristics

The fabricated TiO_2 and Au/TiO_2 materials with different Au content will be studied for their typical physicochemical properties including surface morphology, crystal structure, optical absorption ability thanks to various methods. Physicochemical analysis methods such as X-ray

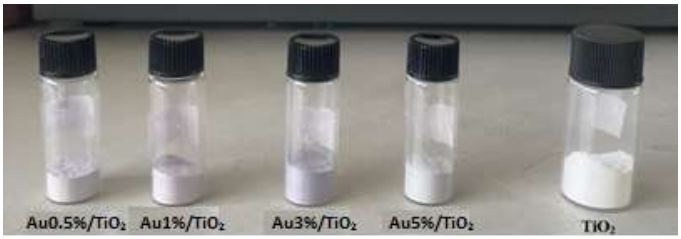

Fig. 2. Photos of TiO_2 and Au/TiO_2 nanocomposite samples with varying contents.

diffraction (Bruker AXS D8 Advance), infrared spectroscopy (FT – IR), scanning electron microscope (SEM), energy dispersive X-ray spectroscopy (EDX), XPS photoelectron, UV-Vis absorption spectra, photoluminescence spectra.

2.3. Photocatalytic activity

Experiments to study the kinetics and evaluate the ability to decompose methylene blue (MB) in water environment of TiO_2, Au/TiO_2 samples with different concentrations were carried out in reaction vessels with the same volume. MB solution is 5 ppm and catalyst content is 20 mg/l. Before the photocatalytic reaction is conducted, the sample will be incubated in the dark for 30 minutes and under UV light for 50 minutes, after which the reaction vessel is illuminated with UV light from a 15 W Philip lamp. The distance from the lamp to the solution surface is 20 cm. The remaining MB concentration in the solution will be determined by the standard curve method using a UV-Vis spectrophotometer at 664 nm wavelength.

3. Results and Discussion

3.1. Infrared spectroscopy FT – IR

Figure 3 presents the FT-IR spectra of TiO_2 and Au/TiO_2 materials with different compositions. The FT-IR spectrum was measured in the wavenumber range from 400 cm^{-1} to 4000 cm^{-1}. The absorption peaks in the range of 3200 cm^{-1} to 3600 cm^{-1} and 1620 cm^{-1} to 1660 cm^{-1} correspond to the valence vibration and deformation vibration of the O-H bond of the adsorbed H_2O molecules, respectively on the surface of the material. A broad absorption region with the maximum peak located at about 715 cm^{-1}, extending from 400 cm^{-1} to about 1000 cm^{-1} is the characteristic absorption region of the Ti-O bond of TiO_2 material.

3.2. X-ray diffraction pattern

Figure 4 shows the X-ray diffraction pattern of the TiO_2 sample prepared by the sol-gel method and the synthesized Au/TiO_2 samples. The peaks of TiO_2 and Au match the JCPDS standard data. First of all, diffraction peaks with relatively large widths can be observed. This proves that the fabricated materials are small in size. Diffraction peaks of Au0.5%/TiO_2 and Au1%/TiO_2 appear at position $2\theta = 25.3°$; 37.9°; 48.1°, 55.1° corresponding to the (101), (004), (200) and (211) lattice planes of the anatase TiO_2 phase. For samples Au3%/TiO_2 and Au5%/TiO_2, an additional peaks of 38.1°; 44.3° and 64.5° correspond to the (111) plane; (200) and (220) face-centered cubic crystal lattice of Au. The signal at 38.1° has very strong intensity, which shows that Au nanoparticles tend to grow strongly toward the (111) plane. Besides, when increasing the Au

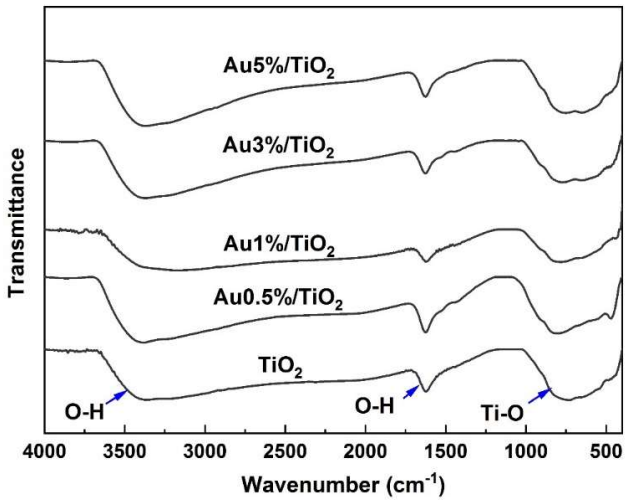

Fig. 3. FT-IR spectra of TiO_2 and Au/TiO_2 nanocomposite materials.

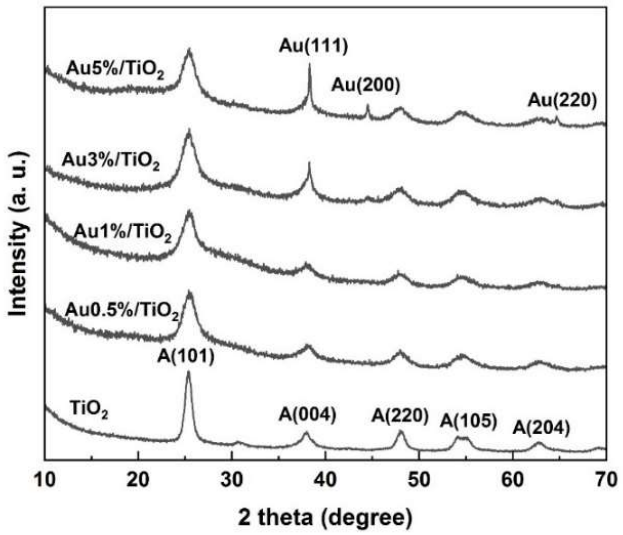

Fig. 4. X-ray diffraction patterns of Au/TiO_2 material with varying contents.

content from 0.5% to 5%, the intensity of the characteristic signal at position 25.3° of TiO_2 tends to decrease. Thus, according to the results of the XRD diagram, when TiO_2 is modified with Au nanometers, the average size of the material will decrease.

3.3. Scanning electron microscope

TiO_2 and Au/TiO_2 materials with different Au content had their surface structure morphology determined by SEM method and are shown in Fig. 5. The structural morphology of the

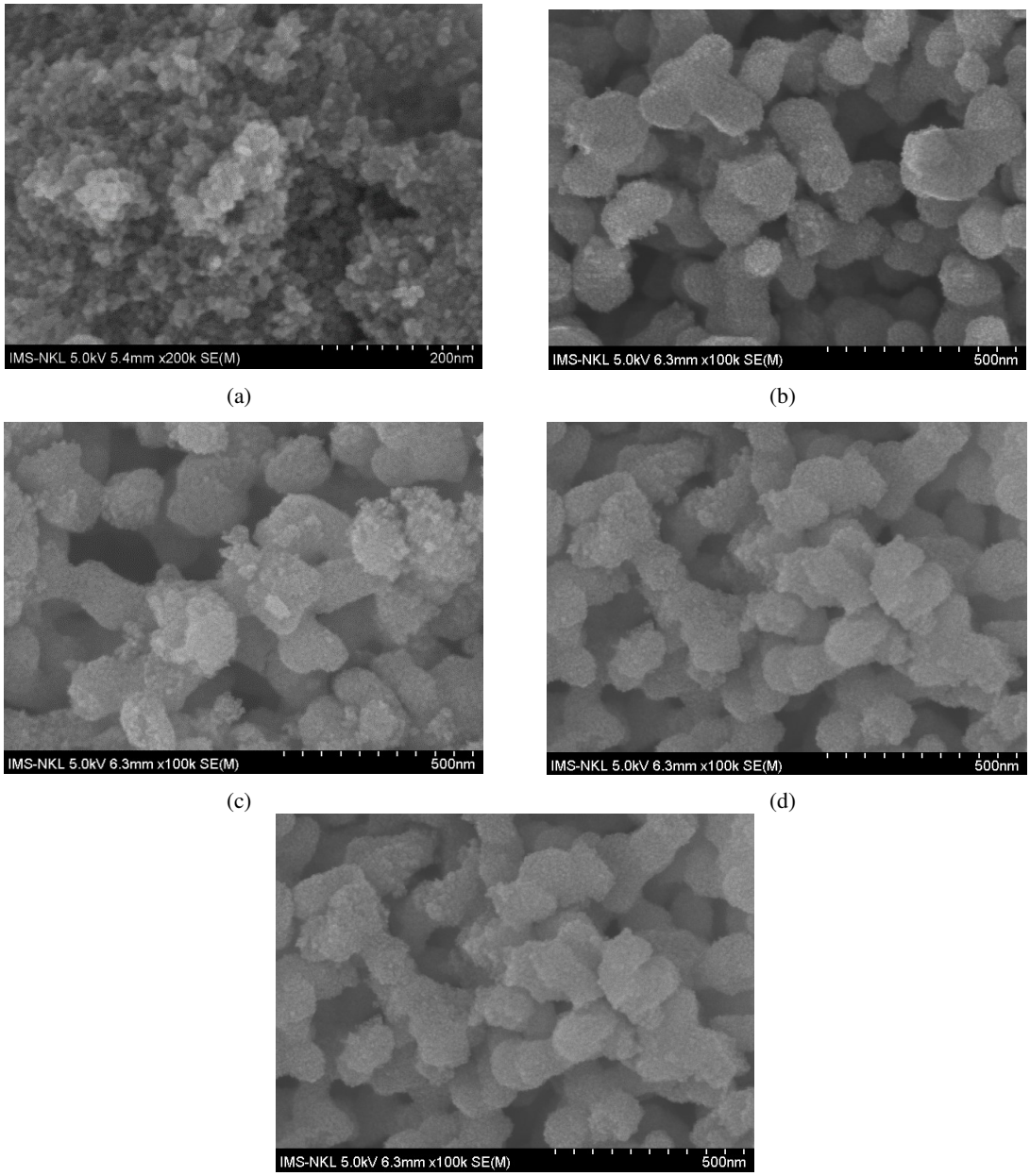

Fig. 5. SEM images of materials (a) pure TiO_2, (b) Au0.5%/TiO_2; (c) Au1%/TiO_2; (d) Au3%/TiO_2 and (e) Au5%/TiO_2.

synthesized materials is shown in Fig. 5. It can be seen that the single-component coating materials TiO_2 and the two-component materials Au/TiO_2 both have a spherical structure. The TiO_2

nanoparticles (Fig. 5a) observed in the image have a relatively small size of about 15-17 nm. For Au/TiO_2 nanocomposite materials, the particle size is much larger, about 150 nm (Fig. 5b, c, d and e) and on the surface, very small Au particles observed are densely distributed on the surface of TiO_2 particles.

The $Au1\%/TiO_2$ material was used as an EDX analysis sample to determine the elemental composition present in the material, and the results are shown in Fig. 6. In the spectrum, signals appear at position 0.4 eV and 4.5 eV, respectively of the Ti element and at a position near 0.45 eV a signal corresponding to the O atom appears. In addition, some low intensity signals appear at position 1.5 eV; 2.1 eV; 8.5 eV and 9.7 eV are typical of the element Au. On the spectrum, no other signals appear, which proves that the Au/TiO_2 materials are made by photochemical reduction method consisting of three elements Ti, O and Au and in addition do not contain any impurities and other substances.

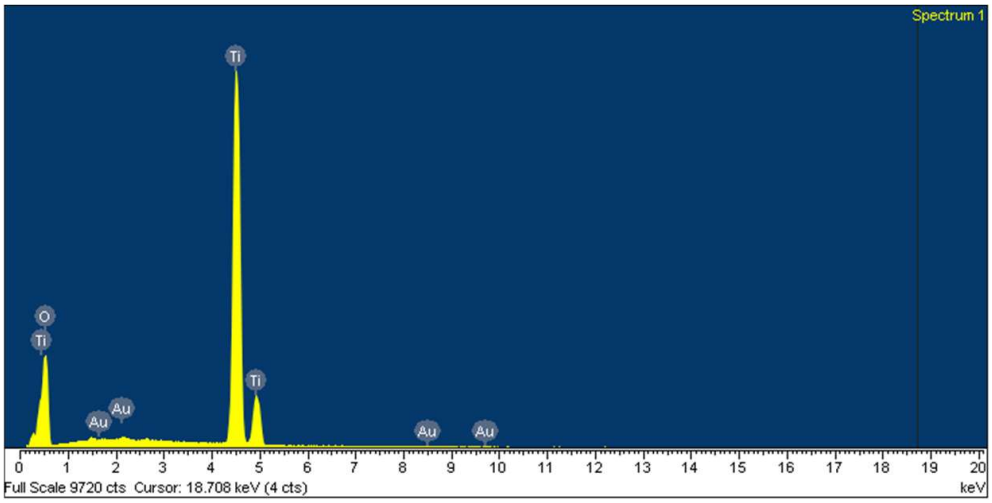

Fig. 6. EDX spectrum of the $Au0.1\%/TiO_2$ material.

3.4. UV-Vis molecular absorption spectrum

To further explore the optical property of all synthesized samples, the light absorption capacity of all synthesized Au/TiO_2 NPs as well as the pure TiO_2 was then analyzed. As illustrated in Fig. 7, the pure TiO_2 NPs exhibited a strong absorbance during the ultraviolet (UV) light regime ($\lambda < 400$ nm) due to its visible light inertness in nature. All Au/TiO_2 NPs exhibited strong absorption spectrum in the visible light region ($\lambda > 450$ nm) with the broad absorption features ~ 500–600 nm, assigning to the LSPR behavior of deposited Au NPs [19]. The intensity of LSPR peaks increased as the increase of nominal gold loading up to 1 wt% and dropped slightly afterward. A high light absorption might enhance the harvesting of incident light and also promote the photocatalytic activity.

3.5. Photoluminescence spectra

Figure 8 shows the PL spectra of pure TiO_2 and $Au1\%/TiO_2$ at room temperature. The pure TiO_2 sample shows a PL peak maximum at $\sim$ 570 nm (black curve). The intensity of the

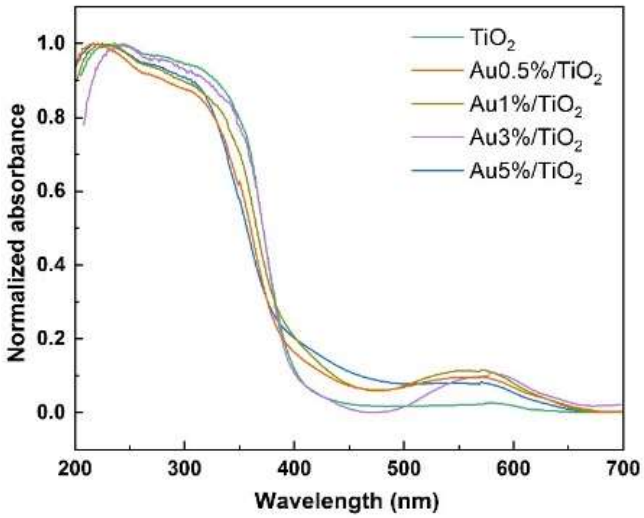

Fig. 7. UV–Vis absorption spectra of TiO2 and Au/TiO2 NPs synthesized at different gold loadings in the range of 0.5–5 wt%.

PL emission of the Au1%/TiO_2 sample is significantly suppressed compared to that of pure TiO_2 (red curve). This result is evidence of Au nanoparticles capturing photoexcited electrons from TiO_2 [20] and supplying a recombination route that does not generate PL. As a result, the probability of excited electrons to radiatively recombine with holes in TiO_2 is strongly suppressed.

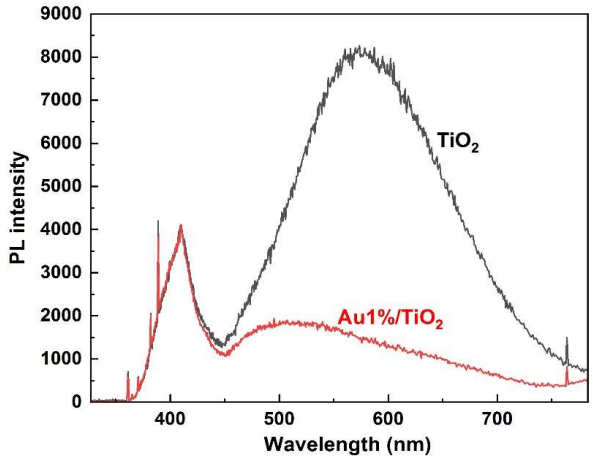

Fig. 8. Photoluminescence spectra of pure TiO_2 (black) and Au/TiO_2 (red) at room temperature.

3.6. X-ray photoelectron spectroscopy

Figure 9 shows the measured spectra of Ti 2p, O 1s, and Au 4f of the material sample. Ti 2p spectrum of reference TiO_2, reduced form Ti^{3+} can be seen at a binding energy $\sim$ 0.6 eV

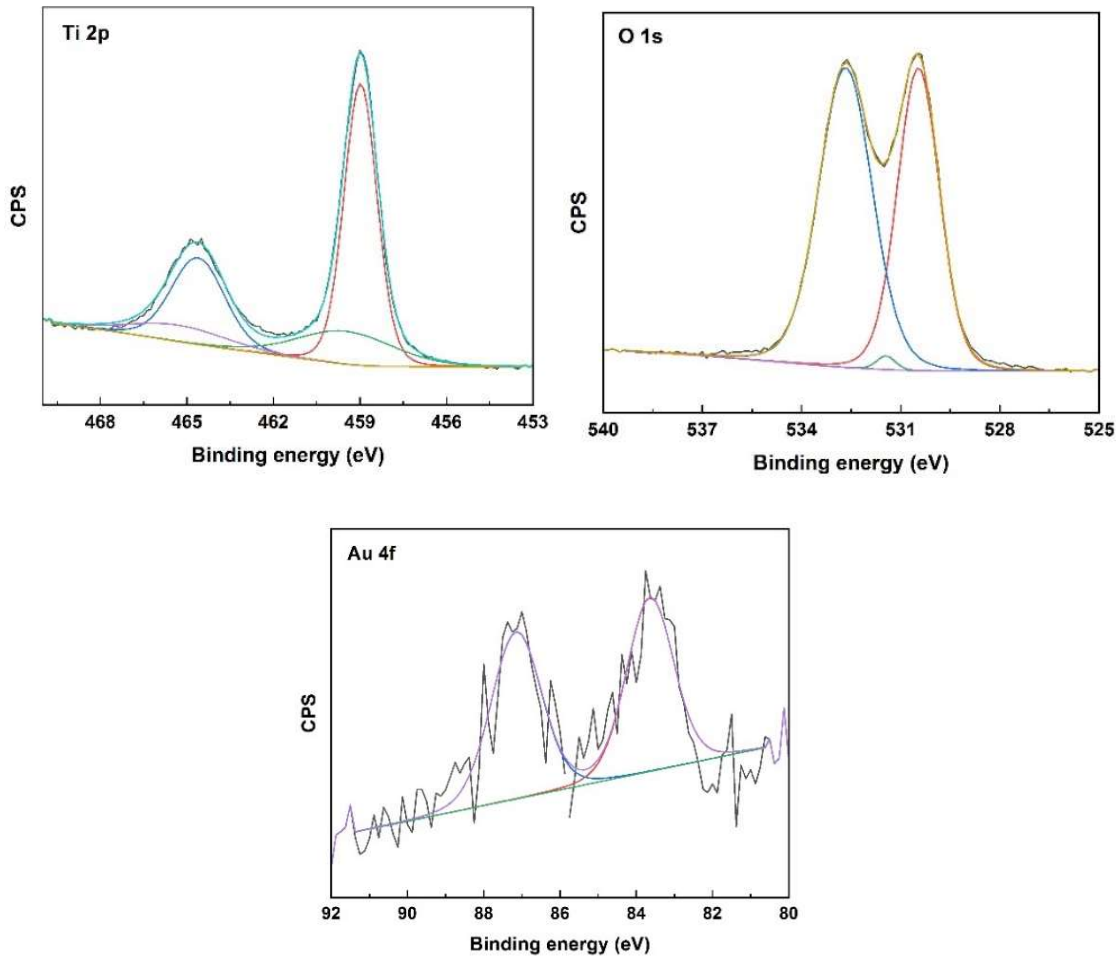

Fig. 9. High resolution XPS spectra of (a) Ti 2p, (b) O 1s and (c) Au 4f for Au/TiO_2 nanocomposite.

above the Ti^{4+} peak with a content of about 33.7%. The high-resolution XPS spectrum of O 1s was deconvoluted into three peaks located at 530.5 eV, 531.5 eV, and 532.6 eV, respectively. The large intense peak centered at 530.5 eV is related to oxygen in the crystal lattice (Ti-O-Ti bond), in which another large intense peak centered at 532.6 eV and a smaller peak at 531.5 eV is attributed to the surface hydroxyl group (Ti-OH) due to oxygen vacancies (OVs) on the surface, indicating the existence of adsorbed hydroxyl groups or water molecules [8–10]. Matching the Au 4f high-resolution XPS spectrum of the Au/TiO_2 material shows that the gold nanoparticles are in only the metallic state.

A Ti^{3+}/Ti^{4+} composition of 0.337 in gold-decorated titanium dioxide (Au/TiO_2) signifies a substantial presence of oxygen defects. These defects, along with the gold nanoparticles, play a pivotal role in enhancing the material's photocatalytic activity by modifying its electronic and optical properties. The presence of trivalent titanium ions (Ti^{3+}) in the titanium dioxide (TiO_2) lattice

is intrinsically linked to the formation of OVs. This is a crucial parameter, as the number of OVs and Ti^{3+} centers profoundly impacts the material's ability to absorb light and separate charge carriers, which are fundamental steps in photocatalysis. The high concentration of separated charge carriers in Au/TiO_2 with a Ti^{3+}/Ti^{4+} ratio of 0.337 leads to a prolific generation of these reactive oxygen species, resulting in a significantly enhanced rate of photocatalytic reactions.

3.7. Photodegradation of methylene blue

The UV-light photocatalytic performance of various Au-modified TiO_2 NPs is shown in Fig. 10. Evaluation of the prepared samples' photocatalytic activities, based on MB degradation over time (Fig. 10a), revealed that the 1 at% gold loading in Au/TiO_2 resulted in the most efficient MB degradation. This was determined by measuring the reduction in the 664 nm peak intensity in the optical absorbance spectra. The rate constant (k) for TiO_2 was 2.75×10^{-2} min^{-1} (Fig. 10b). Notably, the formation of the Au/TiO_2 composite photocatalyst enhanced activity, increasing rate constants from 4.56×10^{-2} min^{-1} to 5.79×10^{-2} min^{-1} (Fig. 10b). 0.5% Au loading on TiO_2 might be below the threshold required to effectively utilize the beneficial roles of Au NPs in photocatalysis, such as efficient charge separation. However, higher gold loadings (3% and 5%) led to decreased photocatalytic activity compared to the 1% sample. This reduction is potentially due to the high gold content facilitating free electron transfer within the gold structure, acting as an electron sink and thus slowing down the process [21]. But excessive gold might cause shadowing, hindering light absorption by the photocatalyst NPs [22, 23]. The photo-catalytic activity of the Au1%/TiO_2 for MB degradation under UV irradiation was also compared with previously reported materials for MB degradation under different irradiation sources (Table 1).

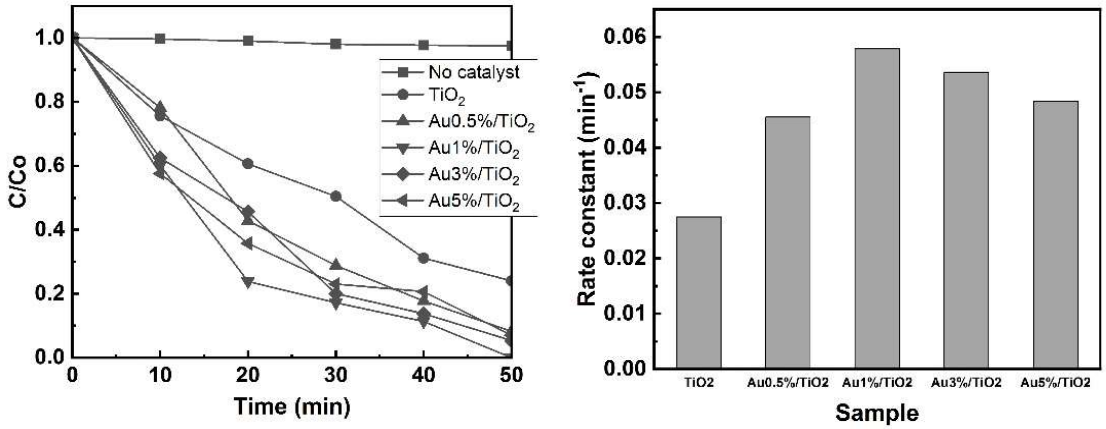

(a) (b)

Fig. 10. (a) Photocatalytic decolorization of MB solution for the TiO_2 and Au/TiO_2 photocatalysts and (b) their corresponding rate constant under UV-light irradiation.

Table 1. Comparison of photocatalytic activity from other works related to Au/TiO_2 or other nanomaterials on MB degradation.

Nanomaterials	**Irradiation source**	Studied degradation time (min)	Concentration of MB (ppm)	Degradation rate (k) min^{-1}	Ref.
TiO_2	Xenon lamp	90	16	3.16×10^{-2}	[24]
Au/TiO_2	UV lamp ($\lambda \geq 254$ nm)	200	2	1.14×10^{-2}	[25]
Ag/TiO_2	UV lamp ($\lambda \geq 254$ nm)	200	2	0.71×10^{-2}	[25]
Cu/TiO_2	UV lamp ($\lambda \geq 254$ nm)	200	2	1.73×10^{-2}	[25]
Au/TiO_2	Halogen lamp as the visible light source	250	2	0.65×10^{-2}	[25]
Ag/TiO_2	Halogen lamp as the visible light source	250	2	0.4×10^{-2}	[25]
Cu/TiO_2	Halogen lamp as the visible light source	250	2	0.55×10^{-2}	[25]
TiO_2	UV (365 nm)	180	10	1,8 x 10^{-2}	[26]
$Fe_3O_4/SiO_2/TiO_2$	UV-C (365 nm)	60	4	4.74×10^{-2}	[27]
$Au@TiO_2$	Xenon lamp	120	30	0.704×10^{-2}	[28]
Au/TiO_2	UV (254 nm)	50	5	5.79×10^{-2}	This work

4. Conclusion

The Au/TiO_2 nanocomposite material was successfully synthesized by the sol-gel method combined with the photochemical reduction process. The deposited Au NPs in the investigated range of 0.5–5 wt%. The process of modifying Au nanoparticles on the surface not only increased the particle size but also significantly effected on the photocatalytic efficiency of the material. The $Au1\%/TiO_2$ nanomaterial had the best ability to decompose MB in aqueous environment, reaching 100% after 50 minutes of UV irradiation.

Acknowledgment

This research is funded by Vietnam Academy of Science and Technology (VAST) under Program for Development of Physics in Vietnam under grant number KHCBVL.04/24-25.

Conflict of Interest

The authors have no conflicts of interest to declare.

References

[1] R. P. Zaccaria, F. Bisio, G. Das, G. Maidecchi, M. Caminale, C. D. Vu *et al.*, *Plasmonic color-graded nanosystems with achromatic subwavelength architectures for light filtering and advanced sers detection*, ACS Appl. Mater. Interfaces **8** (2016) 8024.

[2] V. D. Chinh and N. Q. Trung, *Synthesis and optical properties of colloidal au–ag alloy nanoparticles*, Int. J. Nanotechnol. **12** (2015) 515.

[3] P. K. Jain, X. Huang, I. H. El-Sayed and M. A. El-Sayed, *Review of some interesting surface plasmon resonance-enhanced properties of noble metal nanoparticles and their applications to biosystems*, Plasmonics **2** (2007) 107.

[4] O. K. Orhan and M. Ponga, *Surface-plasmon properties of noble metals with exotic phases*, J. Phys. Chem. C **125** (2021) 21521.

[5] R. Liu, D. Zhan, D. Wang, C. Han, Q. Fu, H. Zhu *et al.*, *Surface plasmon resonance effect of noble metal (ag and au) nanoparticles on bivo4 for photoelectrochemical water splitting*, Inorganics **11** (2023) 206.

[6] H. Aghlara, R. Rostami, A. Maghoul and A. SalmanOgli, *Noble metal nanoparticle surface plasmon resonance in absorbing medium*, Optik **126** (2015) 417.

[7] M. I. Anik, N. Mahmud, A. A. Masud and M. Hasan, *Gold nanoparticles (gnps) in biomedical and clinical applications: A review*, Nano Sel. **3** (2022) 792.
[8] S. Park, V. P. Nguyen, X. Wang and Y. M. Paulus, *Gold nanoparticles for retinal molecular optical imaging*, Int. J. Mol. Sci. **25** (2024) 9315.
[9] G. Rajendran, T. Rajamuthuramalingam, D. M. I. Jesse and K. Kathiravan, *Synthesis and characterization of biocompatible acetaminophen stabilized gold nanoparticles*, Mater. Res. Express **6** (2019) 095043.
[10] N. Wehbe, J. E. Mesmar, R. E. Kurdi, A. Al-Sawalmih, A. Badran, D. Patra *et al.*, *Halodule uninervis extract facilitates the green synthesis of gold nanoparticles with anticancer activity*, Sci. Rep. **15** (2025) 4286.
[11] X. Hu, Y. Zhang, T. Ding, J. Liu and H. Zhao, *Multifunctional gold nanoparticles: A novel nanomaterial for various medical applications and biological activities*, Front. Bioeng. Biotechnol. **8** (2020) 990.
[12] D. K. Das, A. Chakraborty, S. Bhattacharjee and S. Dey, *Biosynthesis of stabilised gold nanoparticle using an aglycone flavonoid, quercetin*, J. Exp. Nanosci. **8** (2013) 649.
[13] V. D. Chinh, I. Bavasso, L. D. Palma, A. C. Felici, M. Scarsella, G. Vilardi *et al.*, *Enhancing the photocatalytic activity of TiO_2 and TiO_2–SiO_2 by coupling with graphene–gold nanocomposites*, J. Mater. Sci.: Mater. Electron. **32** (2021) 5082.
[14] V. D. Chinh, N. Q. Liem, H. S. Cho and S. C. Jeoung, *Relaxation dynamics of photoexcitations in TiO_2 and its composites with au/carbon nanotube (graphene)*, Catal. Commun. **139** (2020) 105970.
[15] V. D. Chinh, L. X. Hung, L. D. Palma, V. T. H. Hanh and G. Vilardi, *Effect of carbon nanotubes and carbon nanotubes/gold nanoparticles composite on the photocatalytic activity of TiO_2 and TiO_2–SiO_2*, Chem. Eng. Technol. **42** (2019) 308.
[16] V. D. Chinh, A. Broggi, L. D. Palma, M. Scarsella, G. Speranza, G. Vilardi *et al.*, *Xps spectra analysis of Ti_2^+, Ti_3^+ ions and dye photodegradation evaluation of titania–silica mixed oxide nanoparticles*, J. Electron. Mater. **47** (2018) 2215.
[17] N. K. Pal and C. Kryschi, *Improved photocatalytic activity of gold decorated differently doped TiO_2 nanoparticles: A comparative study*, Chemosphere **144** (2016) 1655.
[18] A. Orlov, D. A. Jefferson, N. Macleod and R. M. Lambert, *Photocatalytic properties of TiO_2 modified with gold nanoparticles in the degradation of 4-chlorophenol in aqueous solution*, Catal. Lett. **92** (2004) 41.
[19] V. Jovic, W.-T. Chen, D. Sun-Waterhouse, M. G. Blackford, H. Idriss and G. I. N. Waterhouse, *Effect of gold loading and TiO_2 support composition on the activity of au/TiO_2 photocatalysts for h2 production from ethanol–water mixtures*, J. Catal. **305** (2013) 307.
[20] S. M. Kim, S. J. Lee, S. H. Kim, S. Kwon, K. J. Yee, H. Song *et al.*, *Hot carrier-driven catalytic reactions on pt–cdse–pt nanodumbbells and pt/gan under light irradiation*, Nano Lett. **13** (2013) 1352.
[21] Z. Al-Azri, M. AlOufi, A. Chan, G. Waterhouse and H. Idriss, *Metal particle size effects on the photocatalytic hydrogen ion reduction*, ACS Catal. **9** (2019) 3946.
[22] M. Tamura, M. Honda, K. Noro, Y. Nakagawa and K. Tomishige, *Heterogeneous ceo2-catalyzed selective synthesis of cyclic carbamates from CO_2 and aminoalcohols in acetonitrile solvent*, Journal of Catalysis **305** (2013) 191.
[23] X. Zhang, Y. L. Chen, R.-S. Liu and D. P. Tsai, *Plasmonic photocatalysis*, Rep. Prog. Phys. **76** (2013) 046401.
[24] T. V. Chinh, T. T. H. Anh, H. T. C. Tu, H. V. Truong, N. T. H. Phuong, H. P. Hien *et al.*, *Study on photocatalytic degradation of methylene blue by TiO_2 synthesized from titanium slag using a new decomposition agent*, Vietnam J. Catal. Adsorption **11** (2022) 88.
[25] P. Sangpour, F. Hashemi and A. Z. Moshfegh, *Photoenhanced degradation of methylene blue on cosputtered m:TiO_2 (m = au, ag, cu) nanocomposite systems: A comparative study*, J. Phys. Chem. C **114** (2010) 13955.
[26] F. Azeez, E. Al-Hetlani, M. Arafa, Y. Abdelmonem, A. A. Nazeer, M. O. Amin *et al.*, *The effect of surface charge on photocatalytic degradation of methylene blue dye using chargeable titania nanoparticles*, Sci. Rep. **8** (2018) 7104.
[27] C. I. Tarcea, C. M. Pantilimon, E. Matei, A. M. Predescu, A. C. Berbecaru, M. Rapa *et al.*, *Photocatalytic degradation of methylene blue dye using TiO_2 and Fe_3O_4/SiO_2/TiO_2 as photocatalysts*, IOP Conf. Ser.: Mater. Sci. Eng. **877** (2020) 012008.
[28] M. L. Gong, H. T. Fu, X. H. Yang and X. Z. An, *Preparation of au@TiO_2 yolk-shell nanocomposites for solar-light degradation of methylene blue*, IOP Conf. Ser.: Mater. Sci. Eng. **504** (2019) 012016.